Bulk and surface electronic structure of 1T-TiS2 and 1T-TiSe2

Fang, C.M.; Groot, R.A. de; Haas, C.; deGroot, R.A.

Published in:
Physical Review B

DOI:
10.1103/PhysRevB.56.4455

Publication date:
1997

Bulk and surface electronic structure of $1T$-TiS_2 and $1T$-$TiSe_2$

C. M. Fang, R. A. de Groot, and C. Haas
Laboratory of Chemical Physics, Materials Science Center of the University, Nijenborgh 4, 9747 AG Groningen, The Netherlands
(Received 12 December 1996)

Ab initio band-structure calculations were performed for bulk, single slab, and thin films of TiX_2 (X=S, Se) using the localized spherical wave method. According to these calculations, bulk TiS_2 and $TiSe_2$ are semimetallic. The calculations show that TiS_2 thin films are semiconductors, but thin films of $TiSe_2$ are semimetallic. The indirect gap for single slab TiS_2 is about 1.0 eV, and the gap becomes smaller with increasing number of layers. When the number of layers increases to 11, the TiS_2 thin films are semimetallic. All but the surface layers are found to be electrically neutral. The density of states as a function of the energy for the surface layer is different from that of the bulk. The Madelung energy of the Ti atoms on the surface is about 0.35 eV lower than that for the Ti atoms in the bulk. The calculations are compared with photoemission spectra, reported in the literature. [S0163-1829(97)05532-X]

I. INTRODUCTION

This paper addresses three interesting problems concerning the electronic structure of TiS_2 and $TiSe_2$. In the first place, we discuss the problem of whether TiS_2 and $TiSe_2$ are semimetals or semiconductors. Second, we investigate the difference between the electronic structure of the (001) surface layer of a TiS_2 crystal and the bulk. We show that the difference is quite large, and that it has important implications for the interpretation of photoelectron spectra of TiS_2 and $TiSe_2$. Finally, we study the effects of quantum confinement of electrons in a thin slab of TiS_2, and find that a simple slab of TiS_2 is a semiconductor with a band gap of about 1.0 eV.

TiS_2 and $TiSe_2$ crystallize in a simple layer-type structure of the $Cd(OH)_2$-type. The structure consists of sandwich slabs, each slab with two layers of S (Se) atoms, and with Ti atoms in octahedral holes. The bonding between the slabs is very weak, and is determined by van der Waals forces. This is the reason for the large stability of the $|001|$ surface of the slabs. Low-energy electron diffraction and scanning tunneling microscopy studies showed no surface reconstruction.[1] At temperatures below 220 K $TiSe_2$ shows a charge-density wave distortion, leading to a $2a\times 2a\times 2c$ superstructure.[2] $1T$-TiS_2 shows no distortion. In this paper we will refer to a ''layer'' or a ''sandwich'' as an entity comprising a S-Ti-S trilayer, and the phrase ''atomic layer'' for the one-atom-layer case.

The layered compounds TiS_2 and $TiSe_2$ have been intensively investigated for more than three decades, not only because of their technological use in high-energy-density batteries, but also because of their interesting electronic structure.[2,3] The question of whether they are intrinsically semiconducting or semimetallic has presented a challenge to both experimental and theoretical techniques. The early optical experiments on TiS_2 and $TiSe_2$ suggested that both compounds were semiconductors with band gaps of 1–2 eV,[4] the metallic properties of each being attributed to impurities and defects. Takeuchi and Katsuta[5] proposed that the metallic properties are intrinsic, resulting from an overlap of the chalcogen p and titanium d bands. For TiS_2 this view was apparently supported by extensive resistivity experiments on pure samples, which revealed a T^2 dependence over a range of 10–400 K,[6] by studies of the variation of the resistivity, thermopower, and lattice parameters with stoichiometry,[7] and by angle-integrated photoemission experiments which show a long tail in the density of states indicating band overlap or a band gap of not more than 0.1 eV.[8,9] Infrared reflectance spectra show that TiS_2 is a semimetal and has free carriers in excess of $10^{22}/cm^3$.[10,11] Most of the angle-resolved photoemission experiments reported overlapping bands in $TiSe_2$.[1,12–19] In one publication[20] the apparent absence of Se $4p$ holes in the valence band was taken as evidence that $TiSe_2$ is a semiconductor, with a band gap of 0.06 eV. Angle-resolved photoemission of TiS_2 showed the presence of electrons in the Ti $3d$ band, consistent with the observed n-type conductivity.[12–15,21–24] These experimental data did not reveal the presence of holes in the S $3p$ valence band of TiS_2. This was taken as evidence for the semiconducting character of TiS_2, and from the data an energy gap of 0.3 ± 0.2 eV was deduced. In this interpretation, the conduction electrons in the Ti $3d$ band must be due to point defects, i.e., to excess Ti atoms.[25] A problem with this interpretation is that it is not compatible with experimental data for the stoichiometry; the sample was reported to be stoichiometric within 0.5%, but the number of conduction electrons is much larger than corresponds with this number.[15]

In order to clarify the experimental and theoretical pictures for the electronic structure of these compounds, many band-structure calculations have been done. The early non-self-consistent calculations gave gaps that were far too large: 2.0 eV for TiS_2, 3.5 eV for $TiSe_2$;[26] 1.4 eV for TiS_2, 0.5 eV for $TiSe_2$.[27] The later self-consistent calculations have come close to experiment: a 0.23-eV gap for TiS_2, 0.18-eV overlap for $TiSe_2$,[28,29] 0.5-eV overlap for TiS_2;[30] 0.24-eV overlap for TiS_2, 0.55-eV overlap for $TiSe_2$;[31] 0.007-eV overlap for TiS_2.[32] All these calculations are related to the bulk structure and could not fully explain the experimental data on photoemission and transport properties.

TABLE I. Input parameters [lattice parameters, coordinates, empty spheres (Va), and Wigner-Seitz radii R_{WS}] and final electronic configurations. WP represents the Wyckoff position.

(a) $1T$-TiS_2: $a=3.407$ Å, $c=5.6953$ Å				
Atom	WP	Coordinates	R_{WS} (Å)	Electronic configuration
Ti	$1a$	0.0, 0.0, 0.0	1.2067	[Ar] $4s^{0.16}4p^{0.222}3d^{1.86}4f^{0.03}$
S	$2d$	$\frac{1}{3}$, $\frac{2}{3}$, 0.2501	1.7209	[Ne] $3s^{1.92}3p^{4.47}3d^{0.30}$
Va	$1b$	0.0, 0.0, $\frac{1}{2}$	1.2067	$1s^{0.12}2p^{0.15}3d^{0.08}$
(b) $1T$-$TiSe_2$: $a=3.540$ Å, $c=6.008$ Å				
Atom	WP	Coordinates	R_{WS} (Å)	Electronic configuration
Ti	$1a$	0.0, 0.0, 0.0	1.302	[Ar] $4s^{0.23}4p^{0.30}3d^{2.07}4f^{0.03}$
Se	$2d$	$\frac{1}{3}$, $\frac{2}{3}$, 0.2550	1.784	[Ne] $4s^{1.92}4p^{4.27}4d^{0.24}4f^{0.07}$
Va	$1b$,	0.0, 0.0, $\frac{1}{2}$	1.261	$1s^{0.13}2p^{0.17}3d^{0.09}$

This paper presents band-structure calculations using an *ab initio* method for bulk, single slab, and thin films of $1T$-TiX_2 ($X=$S, Se). We find that bulk TiS_2 is, as $TiSe_2$, an intrinsic semimetal. Thin films of TiS_2 are intrinsic semiconductors while thin films of $TiSe_2$ remain semimetallic.

II. BAND-STRUCTURE CALCULATIONS

A. Crystal structure

$1T$-TiX_2 ($X=$S, Se, Te) crystallizes in the $1T$-type $Cd(OH)_2$ structure (space group $P3m1$). One Ti atom is at $1a$ (origin) and two X atoms at $2d$ (1/3,2/3,z) and (2/3,1/3,$-z$), with $z=0.2501(4)$ for TiS_2 and $z=0.255\,04(3)$ for $TiSe_2$.[33,34] The structure consists of X-Ti-X sandwiches, separated in the **z** direction by the so-called van der Waals gap. The Ti atoms are trigonal-antiprismatically coordinated by X atoms. There is one sandwich per unit cell.

B. Details of the calculations

Ab initio band-structure calculations were performed with the localized spherical wave (LSW) method[35] using a scalar-relativistic Hamiltonian. We used local-density exchange-correlation potentials[36] inside space filling, and therefore, overlapping spheres around the atomic constituents. The self-consistent calculations were carried out including all core electrons. Iterations were performed with **k** points distributed uniformly in an irreducible part of the first Brillouin zone (BZ), corresponding to a volume of the BZ per **k** point of the order of 1×10^{-5} Å^{-3}. Self-consistency was assumed when the changes in the local partial charges in each atomic sphere decreased to the order of 10^{-5}.

In the construction of the LSW basis,[35,37] the spherical waves were augmented by solutions of the scalar-relativistic radial equations indicated by the atomic symbols $3s$,$3p$,$3d$, $4s$,$4p$,$3d$, and $4s$,$4p$,$4d$ for S, Ti, and Se, respectively. The internal l summation used to augment a Hankel function at surrounding atoms was extended to $l=3$, resulting in the use of $4f$ orbitals for Ti and Se. When the crystal is not very densely packed, as in the case in the layered structure of the TiX_2, and in particular in the case of thin films, it is necessary to include empty spheres in the calculations. The functions $1s$ and $2p$, and $3d$ as an extension, were used for the empty spheres.

The input for the band-structure calculations of $1T$-TiS_2 and $1T$-$TiSe_2$ is listed in Table I. For the TiX_2 multiple layers, the thin films were constructed by $m+n$ layers with m being the number of sandwiches TiX_2 and n the number of ''sandwiches'' of the empty spheres [n is not less than 3 (about 17 Å)]. The height of one sandwich of the empty spheres was the same as one TX_2 sandwich. All thin films have space-group $P3m1$ (no. 164), the same Wigner-Seitz radii, and the same radii-overlap for the same compound. The Wigner-Seitz radii and empty spheres were determined by the requirement that the pressure 3 PV and the individual contribution to it are minimal. This procedure proves to lead to accurate results as was shown in a comparison with a full-potential method.[38]

C. Bulk $1T$-TiX_2 ($X=$S, Se)

The input parameters and calculated electronic configurations are listed in Table I(a) for $1T$-TiS_2 and Table I(b) for $1T$-$TiSe_2$. Figure 1 shows the first BZ and the high-symmetry points for the structure with space-group $P3m1$. Figures 2–5 show the density of states (DOS) and the dispersion of the energy bands. The energies of the states at Γ are given in Table II.

The calculated hand structures of $1T$-TiS_2 and $1T$-$TiSe_2$ are similar to previous self-consistent calculations.[28–32] For $1T$-TiS_2 the two lowest bands are mainly composed of S $3s$ states (Figs. 2 and 3). The energy of these two bands is between -13.5 to -11.5 eV. Between -5.3 eV and $+0.4$

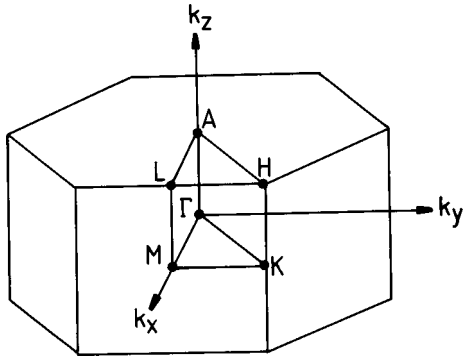

FIG. 1. Brillouin zone and high-symmetry points for $1T$-TiX_2.

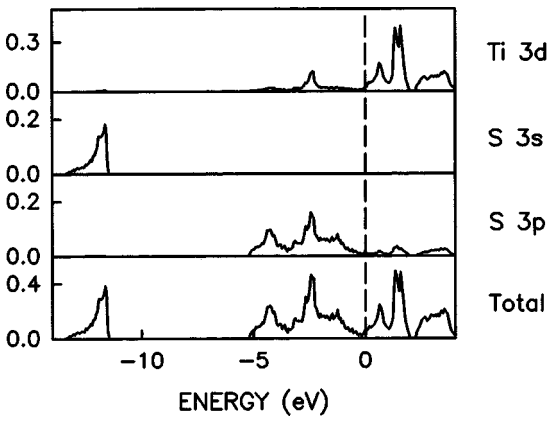

FIG. 2. Total and partial density of states for $1T$-TiS_2.

eV above the Fermi level E_F there are six bands of S $3p$ orbitals. The top and bottom of this set of bands are situated in Γ. Five Ti $3d$ bands of which the crystal-field splitting of an octahedrally coordinated Ti atom (three lower-lying nonbonding t_{2g} and two antibonding e_g states) can be recognized, are above the Fermi level.

It is pointed out that the dispersion of two of the bands in the $\mathbf{k}_z$ direction Γ-A is quite large. These are bands of mainly S $3p_z$ character. The overlap between the S $3p_z$ orbitals within a slab, and also the overlap between S $3p_z$ across the van der Waals gap is quite large, leading to a total band width of about 5 eV. Nevertheless, there is no net bonding across van der Waals gap because both bonding and antibonding states are occupied. (It is worthwhile to note that interactions should not be confused with bonding which is the sum of all interactions.) An indirect overlap of about 0.7 eV exists between the top of the S $3p$ valence band in Γ and the bottom of the Ti $3d$ conduction band situated in L, which agrees with some of the calculations in the literature.[30,31]

We describe briefly, the nature of the wave functions of the S $3p_z$ band, because this will be relevant for the discussion of the electronic structure of the thin films. We use the symmetry labels as given by Miller and Love.[39] The upper S $3p_z$ band (Γ_2^--A_2^+ in Fig. 6) corresponds to states with wave functions which are antibonding within a slab. The maximum of the band (Γ_2^-) is antibonding across the van der

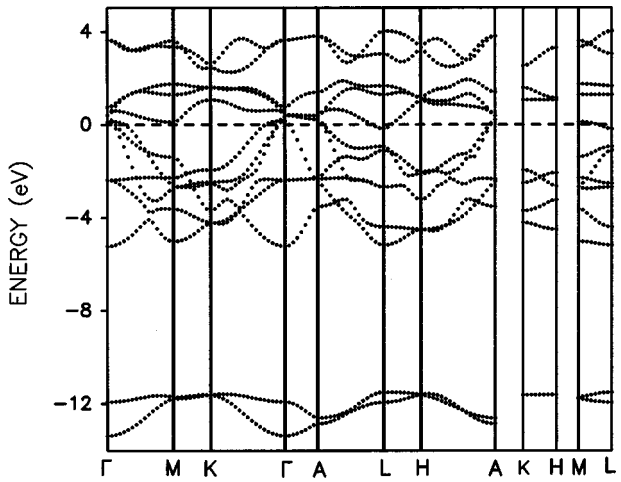

FIG. 3. Dispersion of the energy bands of $1T$-TiS_2.

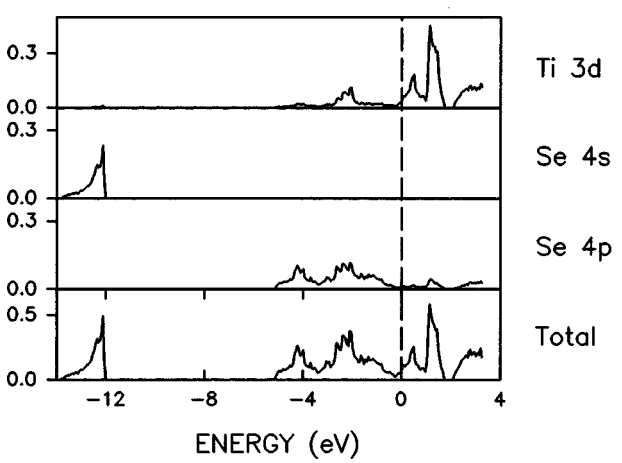

FIG. 4. Total and partial density of states for $1T$-$TiSe_2$.

Waals gap, the minimum (A_2^-) is bonding across the van der Waals gap. The lower S $3p_z$ band (Γ_1^+-A_1^+) is bonding within the sandwich, and bonding (Γ^+) and antibonding (A_1^+) across the van der Waals gap, respectively. The nature of the wave functions is illustrated in Fig. 7.

The band structure of $TiSe_2$ is similar to that of TiS_2. The two Se $4s$ bands are between -13.8 to -12.0 eV. The six Se $4p$ bands are from -5.2 to 0.6 eV above the Fermi level. The bottom and top of the S $3p$ bands are at Γ. The five Ti $3d$ bands are easily recognized. The bottom of the conduction band is at L. There is an overlap of about 0.8 eV at Γ and L.

Near the maximum of the valence band at Γ there are three energy bands with symmetry Γ_2^-, Γ_3^-, and Γ_3^+. A point of controversy in the literature is the topology of these bands, i.e., the ordering of the states Γ_3^+, Γ_2^-, and Γ_3^-. An ordering $E(\Gamma_3^+)>E(\Gamma_3^-)>E(\Gamma_2^-)$ was reported for TiS_2 (Refs. 30 and 31) and $TiSe_2$.[16,29] An ordering $E(\Gamma_3^+)>E(\Gamma_2^-)>E(\Gamma_3^-)$ was reported for TiS_2,[28] and $E(\Gamma_3^-)>E(\Gamma_3^+)>E(\Gamma_2^-)$ for $TiSe_2$.[31] In our calculations we found an ordering $E(\Gamma_3^-)>E(\Gamma_3^+)>E(\Gamma_2^-)$ for TiS_2, and $E(\Gamma_3^-)>E(\Gamma_2^-)>E(\Gamma_3^+)$ for $TiSe_2$. The effects of spin-orbital interaction have been neglected in all calculations. In our opinion, the accuracy of the calculations is not sufficient to establish with certainty the order of the states Γ_3^-, Γ_2^-, Γ_3^+ and the (positive or negative) value of the small energy gap between valence and conduction bands.

The Fermi surfaces of TiS_2 and $TiSe_2$ obtained from our calculations are similar. They are composed of an ellipsoid

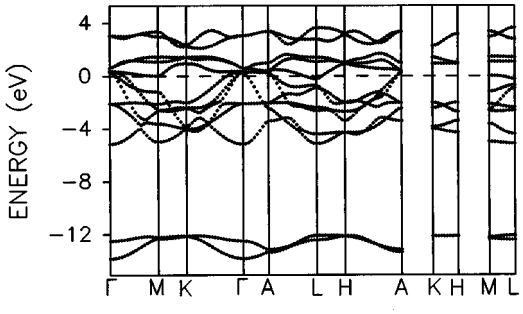

FIG. 5. Dispersion of the energy bands of $1T$-$TiSe_2$.

TABLE II. Energy, dominant orbital character (OC) and symmetry [according to Miller and Love, (Ref. 39)] of the states at Γ for bulk $1T$-TiS_2 and $1T$-$TiSe_2$. Ti $3d^*$ indicates a mix of Ti $3d_{x^2-y^2}$, $3d_{xy}$, $3d_{xz}$, and $3d_{yz}$ orbitals.

$1T$-TiS_2			$1T$-$TiSe_2$		
Energy (eV)	Symmetry	OC	Energy (eV)	Symmetry	OC
−13.38	1+	S $3s$	−13.83	1+	Se $4s$
−11.92	2−	S $3s$	−12.50	2−	Se $4s$
−5.23	1+	S $3p_z$	−5.16	1+	Se $4p_z$
−2.38	3+	S $3p_x$, $3p_y$	−2.10	3+	Se $4p_x$, $4p_y$
0.13	2−	S $3p_z$	0.30	3+	Ti $3d^*$
0.41	3+	Ti $3d^*$	0.32	2−	Se $4p_z$
0.42	3−	S $3p_x$, $3p_y$	0.38	1+	Ti $3d_{z^2}$
0.76	1+	Ti $3d_{z^2}$	0.61	3−	Se $4p_x$, $4p_y$
3.65	3+	Ti $3d^*$	3.06	3+	Ti $3d^*$

around Γ, two cylinders along Γ-A, and one bowl around L. The ellipsoid consists of S $3p_z$ (Se $4p_z$ for $TiSe_2$) states, the two cylinders of S $3p_x$ and S $3p_y$ (or Se $4p_x$ $4p_y$ for $TiSe_2$) states, while the bowl consists of Ti $3d$ states. There are more electron-occupied Ti $3d$ states for $TiSe_2$ than for TiS_2.

In band-structure calculations it is frequently found that the energy gap depends on the Wigner-Seitz (WS) radii and the empty spheres. In the calculations of $1T$-TiS_2, we carried out calculations with different WS radii and with or without empty spheres. It was found that when the number of **k** points is less than 200 the energy gaps depend on the WS radii and on the presence of the empty spheres. When the number of **k** points is larger than 200, that is, if the volume per **k** point is smaller that 6×10^{-5} Å^{-3}, the calculated band structure hardly depends on the WS radii of the atoms or on the presence of the empty spheres.

D. Single slab TiX_2

The electronic structure was calculated for single layers TiX_2 (X=S, Se) separated by three sandwiches of empty spheres ($m=1$, $n=3$). The distance between the slabs is sufficiently large (>17 Å), so that interactions between the slabs are negligible. Since bonding between the layers in the crystal is weak, we do not expect relaxations in the layer at the surface and hence neglect them.

Figures 8 and 9 show the DOS and the dispersion of the energy bands of a single slab of TiS_2. The dispersion of the bands and the DOS of a single slab TiS_2 are similar in many respects with the results obtained for the bulk. This is in agreement with the fact that the main features of the electronic structure are determined by strong covalent intralayer interactions. However, we also observe important differences between single slab and the bulk electronic structure. Whereas, the bulk is semimetallic, with overlapping valence and conduction bands, the single slab is a semiconductor with an indirect energy gap of 1.0 eV. This band gap is not sensitive to the number of k points used in the self-consisted-field cycle and ranges from 0.973 eV for 3/k points to 0.970 eV for 82 k points in the first BZ and beyond. The top of the valence band is at Γ, the bottom of the conduction band is at L. This result is in disagreement with calculations by Umrigar *et al.*[30] who uses the augmented plane wave method, and

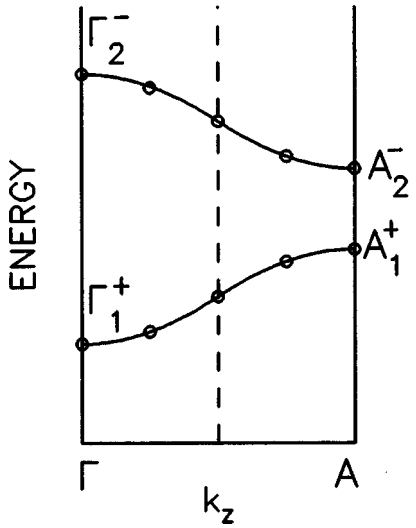

FIG. 6. Dispersion along the $\mathbf{k}_z$ direction of the S $3p_z$ valence bands in bulk TiS_2 and $TiSe_2$. The states for a single slab are represented by the two circles on the broken line, the states for a thin film consisting of five slabs by the ten circles.

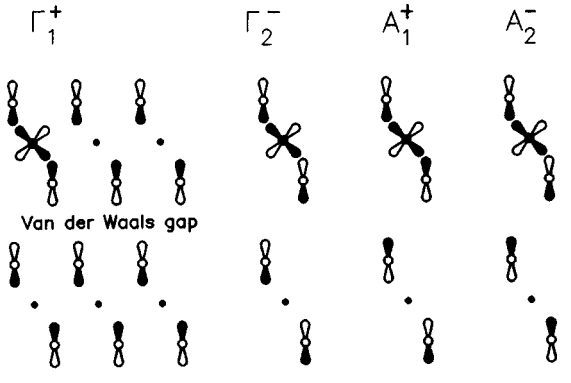

FIG. 7. Sketch of wave functions for a (110) section of $1T$-TiS_2. Open and solid circles represent S and Ti, respectively. On the sulfur atoms the S $3p_z$ orbitals are indicated, the hatched part is a positive sign of the wave-function amplitude, the open part has the negative sign. One of the Ti $3d$ e_g orbitals is also drawn. The phases correspond to the wave functions Γ_1^+, Γ_2^-, A_1^+, and A_2^-.

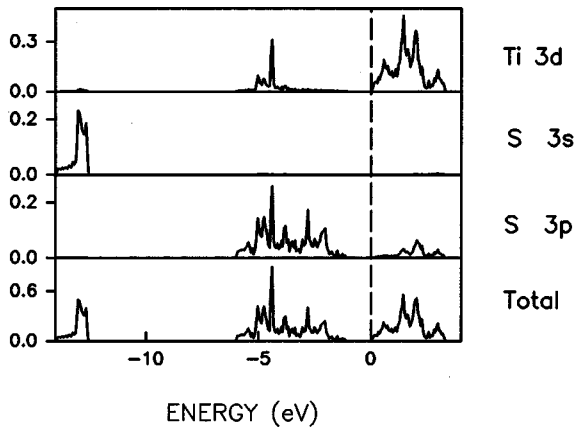

FIG. 8. Total and partial density of states for single slab $1T$-TiS_2.

found only a small difference between the electronic structures of a single slab and the bulk.

The energy difference between bonding and antibonding S $3s$ bands at $\Gamma(A)$ is about 0.9 eV for single slab TiS_2, considerably smaller than the value 1.5 eV for the bulk at Γ. The larger dispersion in the bulk is caused by overlap between S $3s$ orbitals across the van der Waals gap.

The calculations show that in single slab TiS_2 there are 0.28 more electrons within the WS sphere of the Ti atoms than for bulk TiS_2.

Figures 10 and 11 show the dispersion and DOS of single slab $TiSe_2$. The Se $4s$ states are between -13.5 to -12.3 eV. Se $4p$ bands are between -4.24 to 0.03 eV above the Fermi level. The top of the Se $4p$ bands is at $\Gamma(A)$. The lowest Se $4p$ bands are at L, the same as in the case of single slab TiS_2. Five Ti d bands form the conduction bands, which are above the Fermi level except at $L(M)$ where the bands are 0.03 eV below the Fermi level.

There is an important difference between the electronic structures of single slabs of TiS_2 and $TiSe_2$. Whereas a single slab TiS_2 is a semiconductor, there is a small overlap of bands in a single slab $TiSe_2$, so that single slab $TiSe_2$ is semimetallic, just as the bulk. By comparing the dispersion curves for bulk and single slab, we observe that the largest differences are for the S $3p_z$ (Γ_2^-) states, which is strongly lowered in energy in the single slab.

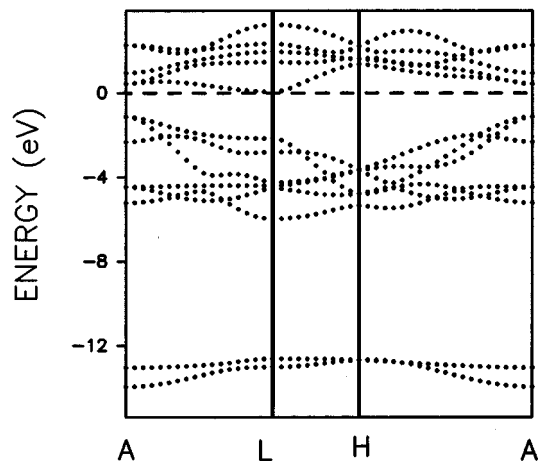

FIG. 9. Dispersion of the energy bands of single slab TiS_2.

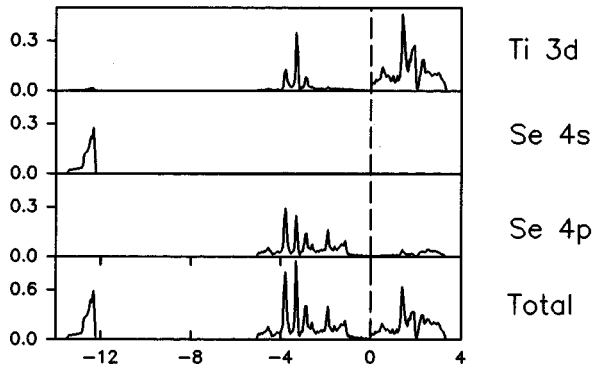

FIG. 10. Total and partial density of states for single slab $TiSe_2$.

E. Thin films

Band-structure calculations were performed for thin films of 5 layers ($m=5$, $n=5$), 7 layers ($m=7$, $n=3$), and 11 layers ($m=11$, $n=3$) of TiS_2.

For the TiS_2 thin films there are more electrons (about 0.02) within the Wigner-Seitz sphere of the Ti atoms of the outer layer as compared with the inner Ti atoms. Similarly, there are less electrons (about 0.02) at the S atoms of the outside atomic layer, as compared to the inner S atoms. The individual sandwiches are neutral, except for the surface one, where the uncompensated spilling out of charge into the vacuum leads to a net positive charge of 0.11 electrons.

Figures 12 and 13(a) show the DOS and the dispersion of the energy bands for a thin film of five layers of TiS_2. The calculations show that the five-layer thin film is a semiconductor with a band gap of 0.26 eV.

The ten S $3s$ bands have an energy between -13.8 to -11.9 eV (compared with -13.9 eV to -12.5 eV in the single layer, and -13.5 eV to -11.5 eV in the bulk). The S $3p$ bands are in the range from -5.6 eV to -0.26 eV below the Fermi level. The lowest position of the S $3p$ bands for the five-layer structure is almost the same as for bulk TiS_2 for Γ and L. Compared with the electronic structure of single-layer TiS_2 every eigenvalue of the S $3p_z$ states at $\Gamma(A)$ is split into five, due to the number of layers. The splitting is a result of the overlap of S $3p_z$ orbitals across the van der Waals gaps in the five-layer thin film. The five levels between -0.6 eV and -2.9 eV correspond to the single state at -2.2 eV for the single slab, and to the upper S $3p_z$ band for the bulk (Γ_2^--A_2^- in Fig. 3). The five levels between -3.7 eV and -5.6 eV correspond to the single state at -5.2 eV

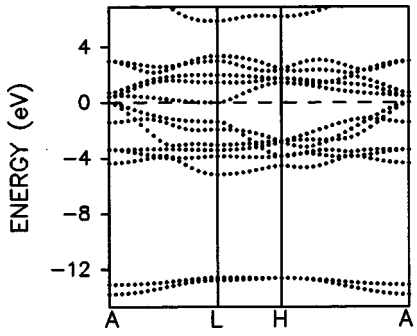

FIG. 11. Dispersion of the energy bands of single slab $TiSe_2$.

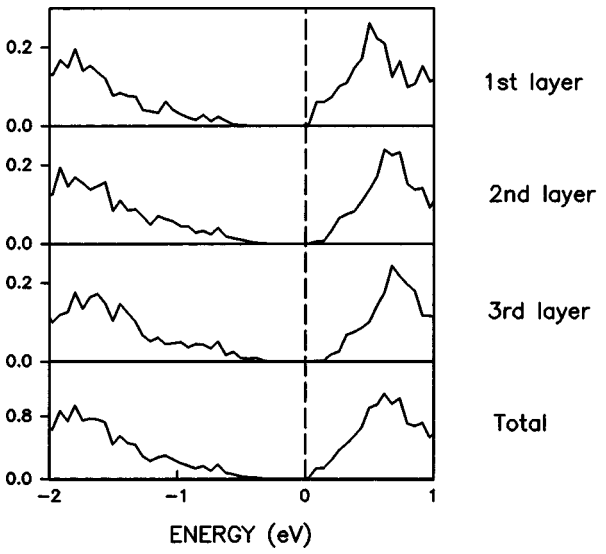

FIG. 12. Total and partial states for a five-layer thin film of TiS_2.

for the single slab and to the lower S $3p_z$ band for the bulk (Γ_1^--A_1^- in Fig. 3). Such a splitting can approximately be described by a simple one-dimensional tight-binding method with overlap matrix elements between S $3p_z$ orbitals across the van der Waals gap, and corresponds to points on the Γ-A dispersion of the bands in the bulk structure (see Fig. 6).

The band structure of five-layer TiS_2 shows an indirect gap of 0.26 eV between $\Gamma(A)$ and $L(M)$, and a direct gap of 0.7 eV at $\Gamma(A)$. The conduction band (Ti d bands) is above the Fermi level. The 15 low-lying nonbonding t_{2g} and 10 antibonding e_g states) are split, as compared with the single-layer structure. The densities of states of the individual layers are represented in Fig. 12. There are small differences, in particular near the Fermi energy. The energy gap of 0.32 eV for the surface layer is larger than the gap of 0.26 eV for the other layers. However, for the surface layer there is a tail of states from the inner layers whose envelope function is expanded in Bessel functions in the outer layer. A very small contribution in the surface DOS originating from bulk envelope functions remains extending to 0.26 eV. For this reason a DOS for thicker slabs is not included. For the outermost layer we find a much steeper increase with energy of the DOS of the Ti $3d$ states. Thus, the lowest states of Ti $3d$ just above the Fermi energy are composed mainly of orbitals of atoms in the outer layer. On the other hand, the highest states of S $3p$ states just below the Fermi energy have a larger contribution orbitals of atoms in the inner layers.

Figure 13(b) shows the dispersion of the energy bands of 11-layer thin films TiS_2 ($m \approx 11$, $n \approx 3$). In this case, we find a splitting of the S $3p_z$ states in two series of 11 states at Γ, due to interlayer overlap across the van der Waals gap. For the 11-layer thin film there is a small overlap of bands, so that this film is semimetallic.

The splitting in subbands [5 or 11 layers of TiS_2 in Figs. 13(a) and 13(b)] is observed throughout the BZ Brillouin zone, but the splitting is generally smaller than it is for the S $3p_z$ states at Γ. In particular the lowest valence-band states at $M(L)$ shows only a very small splitting. This is due to the fact that the wave function of the state is of S $3p_x$, $3p_y$

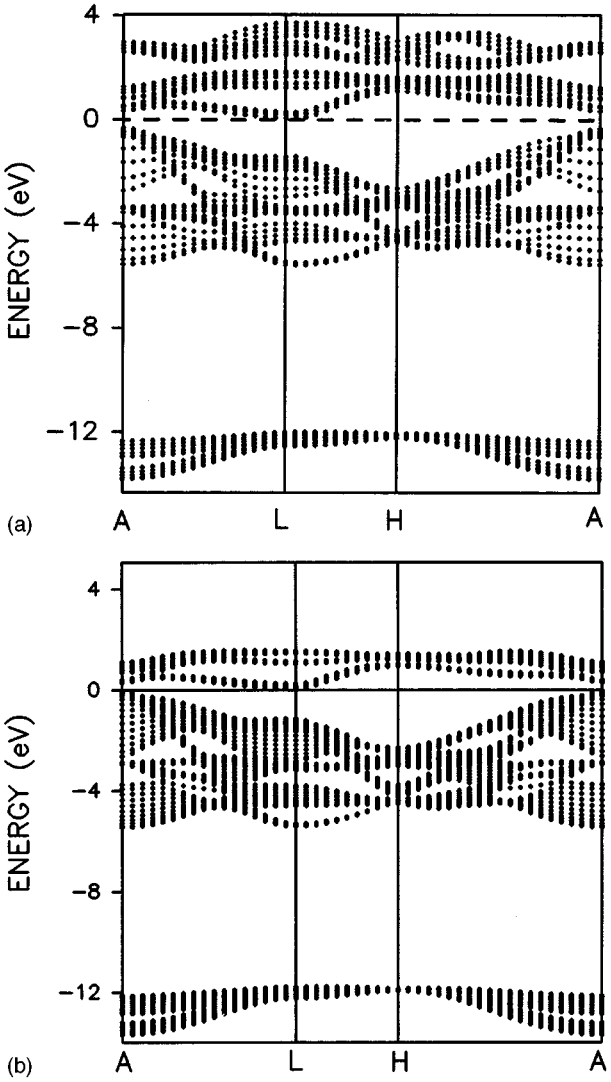

FIG. 13. Dispersion of the energy bands of a five-layer thin film of TiS_2 (a) and of 11-layer thin film of TiS_2 (the bands above 2.0 eV are not included) (b).

character and does not mix with S $3p_z$ states for symmetry reasons. The small splitting at the minimum of the valence band at $M(L)$ must be due to π-type overlap between S $3p_x$, $3p_y$ orbitals across the van der Waals gap; this overlap is apparently quite small.

Figure 14 shows the Madelung energy of the atoms along the **z** (interlayer direction) obtained from the band-structure calculation for a film of 11 slabs. The Madelung energy for atom i with charge Q_i within the WS sphere is given by

$$E_{\mathrm{Mad}}(i) = Q_i \sum_{j \neq i} Q_j / |\mathbf{r}_i - \mathbf{r}_j|;$$

the summation is over all atoms $j \neq i$ in the crystal. As shown in Fig. 14, the Madelung energy is almost the same for all the Ti inner atoms, while the Madelung energy is about 0.35 eV lower for the Ti atom of the outer layer. The Madelung energy is almost the same for all inner S atoms. The E(Mad) of the next to outermost S atoms is about 0.05 eV lower in energy, as compared with the inner S atoms. However, the outermost S atoms have the Madelung energy as

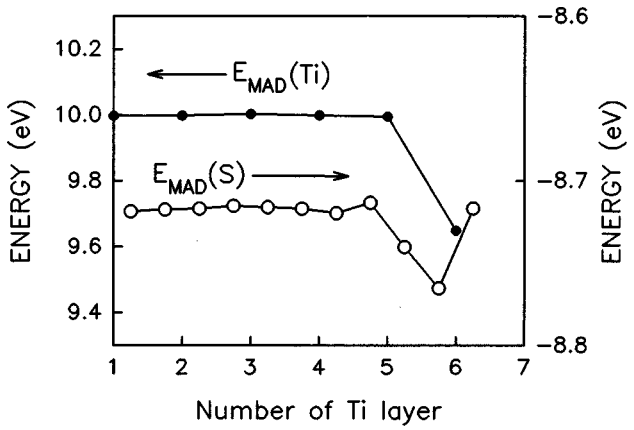

FIG. 14. The Madelung energy (E_{Mad}) of the atoms along the z direction for half of the 11 sandwiches thin films of TiS_2 ($m=11$, $n=3$); the first Ti atom is at the origin (center of symmetry) of the unit cell. The sixth Ti is next to the sandwiches of empty spheres.

high as the inner S atoms. These differences in Madelung energy influence the surface electronic structure.

III. DISCUSSION

From the band-structure calculations we found that bulk $1T$-TiS_2 and $1T$-$TiSe_2$ are semimetals. This result is consistent with electrical transport measurements.

The calculations show that the interlayer interactions of the layered compounds due to overlap between S $3p_z$ orbitals across the van der Waals gap are strong (about 2–3 eV), and have an important effect on the electronic structure. The π-type overlap between S $3p_x$, $3p_y$ orbitals across the van der Waals gap is much smaller.

Due to the lack of three-dimensional (3D) translational symmetry, the chemical bonding and electrostatic interactions of the top layer atoms are different from the bulk. This causes important differences between the electronic structures of the surface and the bulk. For TiS_2 the S $3p$/Ti $3d$ energy gap increases from the bulk to a single slab by about 1.7 eV. This is consistent with the observation that in TiS_2 intercalated with Li, the S $3p$/Ti $3d$ gap has increased by about 1.0 eV,[16,40] because also in this case, the overlap between S $3p_z$ orbitals (across the Li layers) is nearly zero. Generally, one finds that intercalation of metal atoms increases the T nd/S $3p$ gap [e.g., for A_xTS_2 with A=Sn, Pb; T=Ta, Nb, and for ATS_2 (A=Fe, Mn; T=Nb, Ta), by about 1.0–1.5 eV].[40,41]

We compare the width W_π of the S $3p_x$, $3p_y$ band (π-band) of bulk, single slab, and five-layer TiS_2. The width W_π is obtained from the difference between the highest S $3p_x$, $3p_y$ level Γ_3^- and the lowest level at $M(L)$, which is of pure S $3p_x$, $3p_y$ character. The width W_π decreases from 5.46 eV for bulk TiS_2 to values of 5.3 and 4.87 eV for five-layer and a single slab TiS_2, respectively. For $TiSe_2$ W_π decrease from 5.43 eV for the bulk to 5.17 eV for a single slab. Such a decrease of band width is a general phenomenon due to the decrease of overlap contribution of orbitals of surface atoms.

According to the calculations, there is an appreciable change of the total Ti $3d$ band—width W_d (which includes the crystal-field splitting) in going from bulk to thin films. The total Ti $3d$ bandwidth W_d changes from 4.0 eV for bulk TiS_2 to values of 3.75 eV and 3.25 eV for five-layer and single slab TiS_2, respectively. For $TiSe_2$ the values for bulk and surface are 3.73 and 3.33 eV, respectively.

Extensive studies of the photoelectron spectra of TiS_2 and $TiSe_2$ have been reported in the literature, in order to determine the electronic structure and to find out whether TiS_2 and $TiSe_2$ are semiconducting or semimetallic.[1,10–19,32] The angle-resolved photoemission data on TiS_2 are generally in good agreement with the calculated dispersion of the energy bands. The data clearly show the presence of electrons in the Ti $3d$ band near $M(L)$ point in the BZ Brillouin zone, as predicted by band-structure calculations, and in accordance with the observed n-type conductivity. However, the data did not reveal the presence of holes at the top of the valence band near Γ, expected for a semimetal, and predicted by some of the band-structure calculations. Chen *et al.*[15] remarked that the observation that the uppermost S $3p$ band come close to the Fermi energy E_F, but does not cross E_F, indicates that TiS_2 is a semiconductor. However, it is difficult to reconcile this conclusion with experimental data on transport properties, which show large conductivity and a number of charge carriers much larger than corresponding to the stoichiometry of the samples. Weitering[19] observed that photoemission spectra of TiS_2 (001) covered by a thin layer of Ag are very similar to photoemission spectra of a clean TiS_2 (001) surface. The data indicate that the highest occupied valence state of a TiS_2 or an Ag/TiS_2 surface is about 0.2 eV below the Fermi energy. The Fermi energy is pinned by the Ti $3d$ electrons in the conduction band. Generally, these data are taken as evidence for the semiconducting character of pure TiS_2, with an energy gap of about 0.2 eV.

We remark that photoemission spectroscopy is a very surface-sensitive technique. The mean free path λ of electrons escaping from the solid is about 10 Å for photoelectrons with an energy about 20 eV. Because the thickness of a single layer TiS_2 is about 6 Å this means that the photoemission signal originates for a fraction $(1-e^{-\alpha/\lambda})=0.45$ from the outer surface layer, and for a fraction $e^{-\alpha/\lambda}(1-e^{-\alpha/\lambda})=0.27$ from the second layer. Therefore the information obtained from photoelectron spectra concerns mostly the electronic structure of the outer layers of the solid.

Pehlke and co-workers[1,18] have carried out calculations of the photoemission of TiS_2 and $TiSe_2$ using a one-step model for normal electron emission. The calculations show no evidence either for a surface state or a surface resonance. However, it was found that the square-root divergences of the DOS at bulk band-edge disappear for the partial DOS of the surface layer. The calculated photoemission as a function of energy shows important differences if the differences between surface and bulk wave functions are taken into account. The authors stated that this emphasizes the necessity of including surface effects even if there are no surface state or surface resonance.

Our calculations also show the density of states near the Fermi energy of the outer layers of TiS_2 is quite different from the bulk. For the outer layers the DOS of Ti $3d$ states is enhanced, whereas, the DOS of S $3p$ states near the Fermi energy is lower for the outer layers. Thus, due to this difference in electronic structure between surface and bulk, one

expects near the Fermi energy an enhanced photoemission signal for Ti $3d$, and a decreased signal for S $3p$ states. This explains the discrepancies between the observed photoemission spectra and the semimetallic character of TiS_2 quite well. The photoelectron spectrum of semimetallic TiS_2 will look like the photoelectron spectrum of a semiconductor because the electronic structure of the surface layer is similar to that of a semiconductor.

$TiSe_2$ single slab as well as its surface layer is still semimetallic because the effects of broken transitional symmetry are not enough to open an energy gap between Ti $3d$/S $3p$ states, due to the fact that selenium is less electronegative that sulfur.

We discuss briefly the electronic structure and photoemission of $TiTe_2$, which is isomorphous with TiS_2. Bandstructure calculations show that this material is semimetallic.[42,43] Photoemission data[42,43] are in general agreement with the calculated dispersion of the energy bands, but there are some significant differences. The dispersion of the Ti $3d_{z^2}$ band appears to be reduced with respect to band theory. The authors[43] attribute this to Fermi-liquid effects. We like to point out that the change of the partial DOS of the surface layer as compared to the bulk will also lead to an apparent narrowing of the Ti $3d_{z^2}$ band. In the angle-resolved photoemission spectra the Fermi level crossing of the Te $5p_z$ band expected for semimetal was not observed. This might be due to a surface effect, as discussed above for TiS_2.

The large difference between the electronic structure of bulk and single layer TiS_2 is a nice example of quantum confinement. The S $3p_z$ electrons in single layer TiS_2 are confined along the z direction perpendicular to the layers. As a result there is no dispersion along the z direction. Therefore, the S $3p_z$ band, which has a bandwidth and a strong dispersion along z for the bulk TiS_2, becomes a narrow band in single-layer TiS_2. In addition, we observe a significant narrowing of the S $3p_x$, $3p_y$ band. These effects result in a larger band gap of single layer TiS_2 versus semimetallic properties of bulk TiS_2.

Nanostructured materials have recently attracted intense interest at both fundamental aspects and promising applications. This is due to the observation that important changes occur in the physical properties if electrons are confined to nanometer dimensions.[44] The size quantization in cubic CdS and silicon influences the band gap. In order to obtain a smaller band gap in such cubic nanostructured materials it is necessary that all three dimensions are reduced to nanometer size. For layered materials this is not the case. Due to the large anisotropy of the electronic structure it is possible to have a large change of the band gap if only the thickness of the slab of a layered material is reduced to nanometer size.

IV. CONCLUSION

Calculations of the electronic structure of bulk and thin films of TiS_2 indicate that TiS_2 is a semimetal, but that thin films are semiconducting. It is found that the DOS of the outer layer of a thin film is quite different from the bulk: the outer surface layer has an electronic structure similar to that of a semiconductor with a small energy gap and a very small DOS in the gap (originating from the tails of the states of the inner layers). In the literature, photoelectron spectra were taken as evidence that TiS_2 is a semiconductor. However, in the discussion of the data, surface effects were not considered. We have shown that the photoelectron spectra are also consistent with semimetallic TiS_2 if the difference between the electronic structure of the top surface layer and the bulk is taken into account.

ACKNOWLEDGMENTS

We thank Professor Dr. G. A. Wiegers for beneficial discussions and for critical comments on the manuscript, and P. de Boer for help in the calculations. This work was supported by The Netherlands Foundation for Fundamental Research on Matter (FOM).

[1] E. Pehlke and W. Schattke, J. Phys. C **20**, 4437 (1987).
[2] E. Doni and R. Girlanda, in *Electronic Structure and Electronic Transitions in Layered Materials*, edited by V. Grasso (Reidel, Dordrecht, 1986).
[3] J. A. Wilson and A. D. Yoffe, Adv. Phys. **18**, 193 (1969).
[4] D. L. Greenaway and R. Nitsche, J. Phys. Chem. Solids **26**, 1445 (1965).
[5] S. Takeuchi and H. Katsuta, J. Jpn. Inst. Met. **34**, 758 (1970).
[6] A. H. Thompson, Phys. Rev. Lett. **35**, 1786 (1975).
[7] A. H. Thompson, H. R. Pisharody, and R. F. Koehler, Phys. Rev. Lett. **29**, 163 (1972).
[8] P. M. Williams and F. R. Shepherd, J. Phys. C **6**, 136 (1973).
[9] D. W. Fischer, Phys. Rev. B **8**, 3576 (1973).
[10] G. Lucovsky, R. M. White, J. A. Benda, and J. F. Revelli, Phys. Rev. B **7**, 3859 (1973).
[11] R. M. White and G. Lucovsky, Solid State Commun. **11**, 1369 (1972).
[12] R. Z. Bachrach, S. Skibowski, and F. C. Brown, Phys. Rev. Lett. **37**, 40 (1076).
[13] N. V. Smith, J. E. Rowe, and F. J. DiSalvo, Phys. Rev. B **17**, 1836 (1978).
[14] G. Margaritondo, C. M. Bertoni, J. H. Weaver, F. Levy, N. G. Stoffel, and A. D. Katnani, Phys. Rev. B **23**, 3765 (1981).
[15] C. H. Chen, W. Fabian, F. C. Brown, K. C. Woo, B. Davies, B. Delong, and A. H. Thompson, Phys. Rev. B **21**, 615 (1980).
[16] O. Anderson, R. Manzke, and M. Skibowski, Phys. Rev. Lett. **55**, 2188 (1985).
[17] E. Pehlke and W. Schattke, Z. Phys. B **66**, 31 (1987).
[18] E. Pehlke, W. Schattke, O. Anderson, R. Manzke, and M. Skibowski, Phys. Rev. B **41**, 2982 (1990); E. Pehlke, D. Samuelsen, and W. Schattke, Vacuum **41**, 550 (1990).
[19] H. H. Weitering, Ph.D. thesis, Groningen, 1991.
[20] N. G. Stoffel, S. D. Kevan, and N. V. Smith, Phys. Rev. B **31**, 8049 (1985).
[21] C. G. Slough, B. Giambattista, A. Johson, W. W. McNairy, C. Wang, and R. V. Coleman, Phys. Rev. B **37**, 6571 (1988); J. Barry, H. P. Hughes, P. C. Klipstein, and R. H. Friend, J. Phys. C **16**, 393 (1983).

[22] R. H. Friend, D. Jerome, W. Y. Liang, J. C. Mikkelsen, and A. D. Yoffe, J. Phys. C **10**, L705 (1977).
[23] E. M. Logothesis, W. J. Kaiser, C. A. Kukkonen, S. P. Faile, R. Colella, and J. Gambold, J. Phys. C **12**, L251 (1979).
[24] C. A. Kukkonen, W. J. Kaiser, E. M. Logothesis, B. J. Bluemenstock, P. A. Schroeder, S. P. Faile, R. Colella, and J. Gambold, Phys. Rev. B **24**, 1691 (1981); P. C. Klipstein and R. H. Friend, J. Phys. C **17**, 2713 (1984).
[25] J. A. Wilson, Phys. Status Solidi B **86**, 11 (1978).
[26] R. B. Murry and A. D. Yoffe, J. Phys. C **5**, 3038 (1972).
[27] H. W. Myron and A. J. Freeman, Phys. Rev. B **9**, 481 (1974).
[28] A. Zunger and A. J. Freeman, Phys. Rev. B **16**, 906 (1977).
[29] A. Zunger and A. J. Freeman, Phys. Rev. B **17**, 1839 (1978).
[30] C. Umrigar, D. E. Ellis, D.-S. Wang, H. Krakauer, and M. Posternak, Phys. Rev. B **26**, 4935 (1982).
[31] G. A. Benesh, A. M. Woolley, and C. Umrigar, J. Phys. C **18**, 1595 (1985).
[32] J. Dijkstra, C. F. van Bruggen, and C. Haas, J. Phys. Condens. Matter **1**, 4297 (1989).
[33] C. Riekel, J. Solid State Chem. **17**, 389 (1976).
[34] R. R. Chianelli, J. C. Scanlon, and A. H. Thompson, Mater. Res. Bull. **10**, 1379 (1975).
[35] H. van Leuken, A. Lodder, M. T. Czyżyk, F. Springelkamp, and R. A. de Groot, Phys. Rev. B **41**, 5613 (1990).
[36] L. Hedin and B. I. Lundqvist, J. Phys. C **4**, 2064 (1971).
[37] O. K. Anderson and O. Jepsen, Phys. Rev. Lett. **53**, 2571 (1984); O. K. Andersen, Phys. Rev. B **8**, 3060 (1975).
[38] M. Heinemann, H. J. Terpstra, C. Haas, and R. A. de Groot, Phys. Rev. B **52**, 11 740 (1995).
[39] S. C. Miller and W. F. Love, *Tables of Irreducible Representations of Space Groups and Representations of Magnetic Space Groups* (Pruett Press, Boulder, 1967).
[40] J. V. Macanny, J. Phys. C **12**, 3263 (1979); C. M. Fang, G. A. Wiegers, A. Meetsma, R. A. de Groot, and C. Haas, Physica B **226**, 259 (1996).
[41] J. Dijkstra, P. J. Zijlema, C. F. van Bruggen, C. Haas, and R. A. de Groot, J. Phys.: Condens. Matter **1**, 6363 (1989).
[42] D. K. G. de Boer, C. F. van Bruggen, G. W. Bus, R. Coehoorn, C. Haas, G. A. Sawatzky, H. W. Myron, D. Norman, and H. Padmore, Phys. Rev. B **29**, 6797 (1984).
[43] R. Claessen, R. O. Anderson, G. H. Gweon, J. W. Allan, W. P. Ellis, C. Janowitz, C. G. Olson, Z. X. Shen, V. Eyert, M. Skibowski, K. Friemelt, E. Buscher, and S. Hüfner, Phys. Rev. B **54**, 2453 (1996).
[44] G. A. Ozin, Adv. Mater. **4**, 612 (1992).